Study of speckle statistics using modulated apertures

A. M. HAMED

Physics Department, Faculty of Science, Ain Shams University, Cairo, Egypt.

Moments of the intensity distribution in a speckle pattern are calculated using optical systems provided with modulated apertures. A polychromatic light of limited bandwidth is used for the illumination of the optical system. Two different types of modulated apertures are considered. The first type has a rectangular shape, while the second type consists of concentric annuli with black and transparent areas of equal widths. The results are graphically represented in both cases and compared with the results obtained using circular aperture.

1. Introduction

When a rough surface is illuminated with partially coherent light, the reflected beam consists of random patterns of bright and dark regions known as speckle. These patterns have been interpreted in terms of Huygen's principle whereby the intensity at a field point is caused by the interference of wavelets, scattered from different points within the illuminated area, with their phases randomized by height variations of the surface.

The pioneer works on statistical properties of speckle patterns produced by using monochromatic light propagating through a diffuser of limited circular aperture are those of GOODMAN [1], [2], ENLOE [3], and DAINTY [4], [5]. ELBAUM *et al.* [6], BARAKAT [7] and SPRAGUE [8] used light of limited bandwidth to measure surface roughness parameters, while FUJI *et al.* [9] obtained information about the temporal coherence of the light source using speckle interferometry. Also, they and others ([10]−[16]) studied the effect of the object roughness properties on the speckle patterns produced in both image and diffraction fields of the object. An approach to determination of the statistical properties of speckle by means of using light of limited bandwidth is represented by PARRY [17]. He has discussed some effects of temporal coherence on the first order statistics of speckle considering optical system provided with uniform circular aperture. PEDESEN [18]−[20] obtained the contrast of polychromatic speckle patterns and showed its dependence on surface roughness He also studied the second order statistics of speckle formed from the diffracted light using Gaussian rough surfaces [21].

The purpose of this work is to show the effect of the optical system provided with modulated apertures upon the spatial speckle pattern in both cases of modulation. The results of the normalized standard deviation $\sigma/\langle I \rangle$ in the case of modulation are compared with the corresponding results obtained in the case of uniform circular

aperture. In the following section, a theoretical analysis is presented. Then, the results are discussed and, finally, a conclusion is given.

2. Theoretical analysis

It was previously shown [17] that the intensity distribution in the speckle pattern at a point (ξ, η) is given by

$$I(\xi, \eta) = \int_0^\infty S(\lambda) I(\xi, \eta, \lambda) d\lambda \tag{1}$$

where $S(\lambda)$ is the intensity of incident polychromatic light of wavelength λ. The diffuser was limited by a uniform circular aperture and spatially coherent light of limited bandwidth. $I(\zeta, \eta, \lambda)$ is the intensity at the point (ξ, η) in the monochromatic speckle pattern produced by light of wavelength λ. Referring to Fig. 1, the diffuser is considered as a random phase object represented as follows:

$$g(x, y) = U_0(x, y) \exp(-jkz), \quad j = \sqrt{-1} \tag{2}$$

where: $k = 2\pi/\lambda$ is the propagation constant and z is the random optical path, and $U_0(x, y)$ is the complex amplitude of light incident on the diffuser. Hence, the far-field speckle pattern is obtained by operating the Fourier transform upon the diffuser function limited by an aperture $A(x, y)$, i.e.,

$$U(\xi, \eta) = \text{F.T.}[g(x, y)A(x, y)]$$

$$= \frac{1}{j\lambda D} \int\!\!\int_{-\infty}^{\infty} g(x, y)A(x, y)\exp[-(2\pi j/\lambda D)(x\xi + y\eta)]dxdy. \tag{3}$$
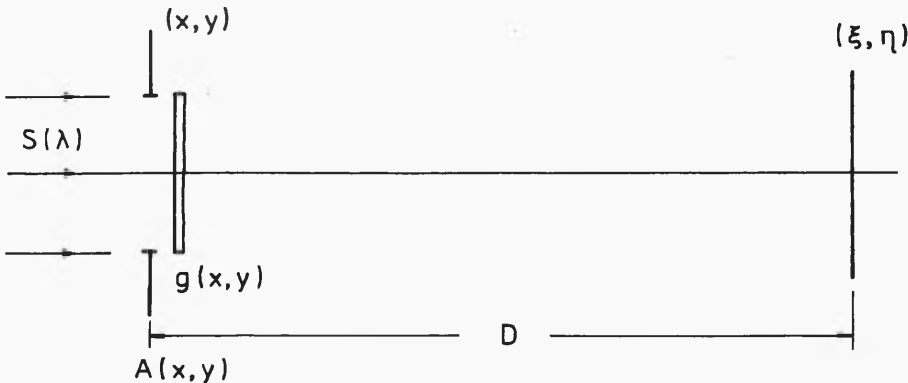

Fig. 1. Diffuser $g(x, y)$ is limited by an apodized aperture $A(x, y)$ consisting of B/W concentric annuli. The statistics are considered in the far-field plane (ξ, η). D — distance between the diffuser and the speckle plane

We assume a one-dimensional rectangular aperture represented as follows:

$$A(x, y) = 1, \quad \text{for } |x/a| \leqslant 1,$$
$$= 0, \quad \text{otherwise.} \tag{4}$$

Substituting from (2), (4) into (3), we obtain

$$U(\xi, \eta) = \iint_{-a}^{a} U_0(x, y) \exp(-jkz) \exp[-(2\pi j/\lambda D)(x\xi + y\eta)] dx dy. \tag{5}$$

The autocorrelation function $C_I(\xi, \eta, \xi', \eta')$, using a theorem due to REED [22], is obtained as follows:

$$C_I(\xi, \eta, \xi', \eta') = \iint_0^{\infty} S(\lambda) S(\lambda') |\langle U(\xi, \eta, \lambda) U^*(\xi + \xi', \eta + \eta', \lambda') \rangle|^2 d\lambda d\lambda'. \tag{6}$$

The variance $\sigma^2[I(\xi, \eta)]$ can be deduced from the autocorrelation function $C_I(\xi, \eta, \xi', \eta')$ by inserting $\xi' = \eta' = 0$ into Eq. (6), hence we get

$$\sigma^2[I(\xi, \eta)] = S(\lambda) S(\lambda') |\langle U(\xi, \eta, \lambda) U^*(\xi, \eta, \lambda') \rangle|^2 d\lambda d\lambda'. \tag{7}$$

Substituting from Equation (5) into Equation (7), and writing $\lambda = 1/v$, we get

$$\sigma^2[I(\xi, \eta)] = \frac{1}{D^4} \iint_0^{\infty} S(1/v) S(1/v') |\langle \exp - 2\pi j z(v - v' \rangle|^2$$

$$|\iint_{-a}^{a} S(x, y) \exp[-2\pi j/D)(v - v')(x\xi + y\eta)] dx dy|^2 dv dv' \tag{8}$$

where $S(x, y) = |U_0(x, y)|^2$ is the intensity distribution in the plane (x, y). Normalizing the above expression by considering the ratio of the standard deviation to the mean intensity, namely $\sigma/\langle I \rangle$, we finally get this result for the rectangular aperture

$$\sigma/\langle I \rangle = \left\{ \frac{4}{2\pi(\sigma_z/\beta)} \int_0^{2\pi(\sigma_z/\beta)} \exp(-x'^2) \left[\frac{\sin(ar'x'/2\pi D\sigma_z)}{ar'x'/2\pi D\sigma_z)} \right]^2 dx' \right\}^{1/2} \tag{9}$$

where the incident light contains all wavelengths in the range from λ_1 to λ_2 with equal intensity and $r' = \sqrt{\xi^2 + \eta^2}$ is the radial coordinate in the speckle plane (ξ, η). $\beta = \lambda_1 \lambda_2/(\lambda_2 - \lambda_1)$ is the spectral bandwidth. It should be noted that Eq. (9) is obtained from Eq. (8) considering that [17]

$$\langle \exp - 2\pi j z(v - v') \rangle = \exp - (2\pi)^2 \sigma_z^2 (v - v')^2/2$$

where σ_z is the standard deviation of the fluctuations in the medium.

It is clear that the ratio $\sigma/\langle I \rangle$ is a function of the far-field coordinate r', hence the statistics is non-stationary considering that the bandwidth β and the r.m.s. surface roughness σ_z are parameters, *i.e.*,

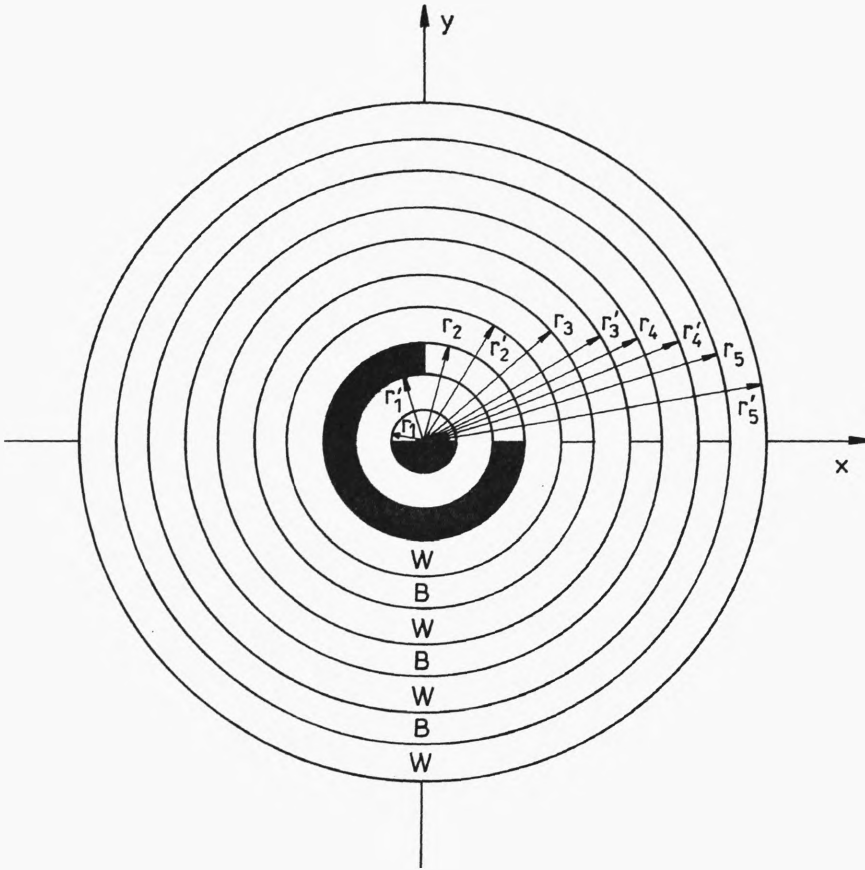$$\sigma/\langle I \rangle = f(r', \beta, \sigma_z).$$

Fig. 2. *B/W* concentric annuli used as an aperture limiting the diffuser. It consists of ten annuli, where only five are transparent

Now, we consider the second type of modulated aperture. It consists of concentric annuli with black and transparent areas of equal widths as shown in Fig. 2. This aperture [23] is represented as follows:

$$A(\rho) = \sum_{i=1}^{N} \Delta A_i \tag{10}$$

where: $\Delta A_i = A_{\rho_i'} - A_{\rho_i}$ is the difference between two successive circular apertures and is considered as an annulus of radial width $\Delta r = r' - r$, N is the total number of transparent and black zones constituting the whole aperture, $\rho = \sqrt{x^2 + y^2}$ is the radial coordinate. The computations are made considering only ten annuli of serial *B/W* equal widths, namely five zones are transparent (white) and the other five zones are opaque.

It is easy to operate the Fourier transform upon Equation (10), using radial coordinates, to obtain this result for the point spread function (PSF)

$$\text{PSF} = \sum_{i=1}^{N} \left\{ \left[\frac{2J_1(w_i')}{w_i'} \right] - \left[\frac{2J_1(w_i)}{w_i} \right] \right\}. \tag{11}$$

Substituting into Equation (3) and following the same analysis, we finally get this result

$$\sigma/\langle I \rangle = \left\{ \frac{4}{2\pi(\sigma_z/\beta)} \int_0^{2\pi(\sigma_z/\beta)} \exp(-x'^2) \left(\sum_{n=1}^{N} \left\{ a_n'^2 \left[\frac{2J_1(w_n')}{w_n'} \right] - a_n^2 \left[\frac{2J_1(w_n)}{w_n} \right] \right\} \right)^2 dx' \right\}^{1/2} \tag{12}$$

where: $w_n' = a_n' r'x/2\pi D\sigma_z$ and $w_n = a_n r'x/2\pi D\sigma_z$ are the reduced coordinates in the speckle plane r'. Equations (9), (12) are numerically solved using electronic digital computer and the theoretical results are presented in the following section.

3. Results and discussion

The results of the normalized $\sigma/\langle I \rangle$ as a function of the radial coordinate r' of the far-field speckle pattern are represented as shown in Fig. 3. In this figure, two curves are shown using rectangular aperture to limit the diffuser, where the lower curve is plotted for r.m.s. surface roughness $\sigma_z = 5$ µm, while the upper curve is plotted for $\sigma_z = 10$ µm. Also, Figs. 4 and 5 show other curves at $\sigma_z = 15$ µm, 25 µm, and
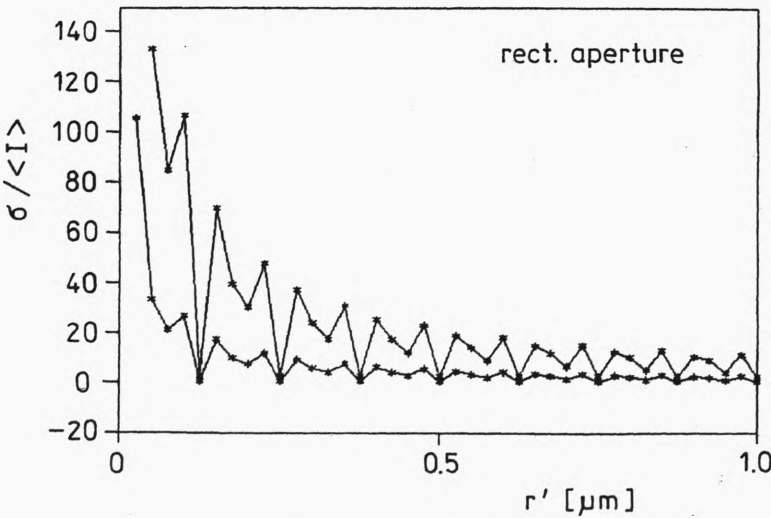

Fig. 3. Normalized values of $\sigma/\langle I \rangle$ vs. the radial coordinate r' [µm] for the far-field speckle pattern, where the lower curve is plotted for $\sigma_z = 5$ µm, and the upper curve is plotted for $\sigma_z = 10$ µm. The spectral BW = 10 nm, and NA = 0.5 is the numerical aperture of the diaphragm that limits the diffuser

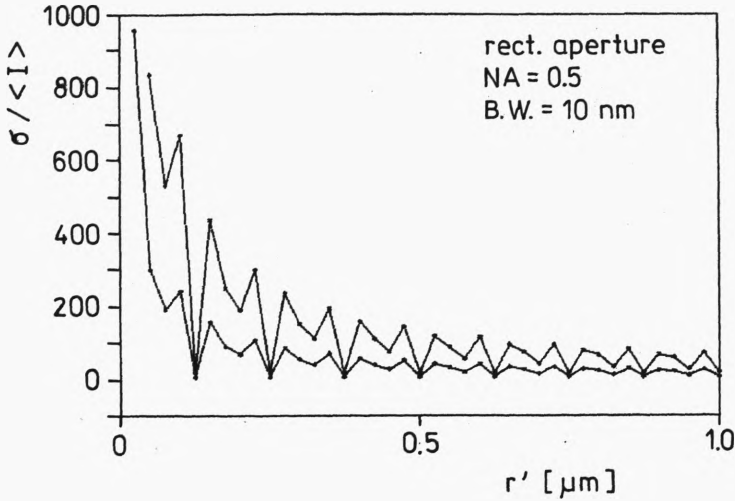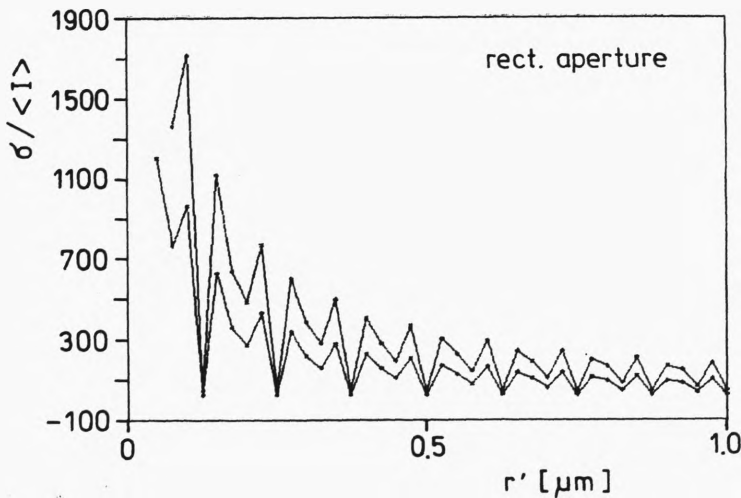Fig. 4. Two different curves of the normalized intensity $\sigma/\langle I \rangle$ vs. the radial coordinate r' [μm] of the far-field speckle pattern, where the lower curve is plotted for $\sigma_z = 15$ μm, and the upper curve is plotted for $\sigma_z = 25$ μm. NA — numerical aperture of the diaphragm that limits the diffuser

Fig. 5. Two different curves of the normalized intensity $\sigma/\langle I \rangle$ vs. the radial coordinate r' [μm] of the far-field speckle pattern, where the lower curve is plotted for $\sigma_z = 30$ μm, while the upper curve is plotted for $\sigma_z = 40$ μm, BW = 10 nm, and NA = 0.5 is the numerical aperture of the diaphragm that limits the diffuser

$\sigma_z = 30$ μm, 40 μm, respectively. Also, two sets of four different curves each are plotted, where the first set has r' ranges from 0 up to 0.5 μm, as shown in Fig. 6, while the second set of curves is constructed in the range from $r' = 0.5$ up to 1.0 μm. The spectral bandwidth $\beta = 10$ nm. It is shown, referring to the above results of
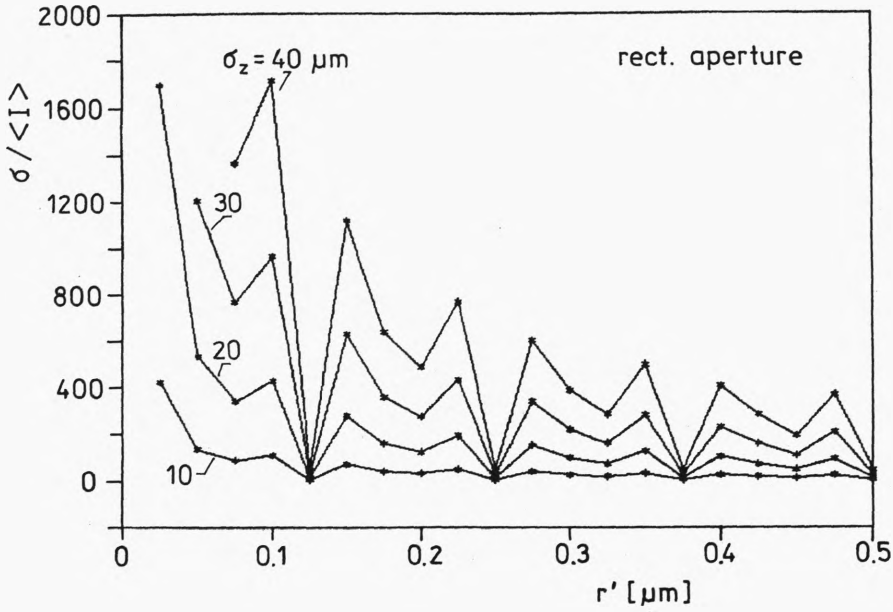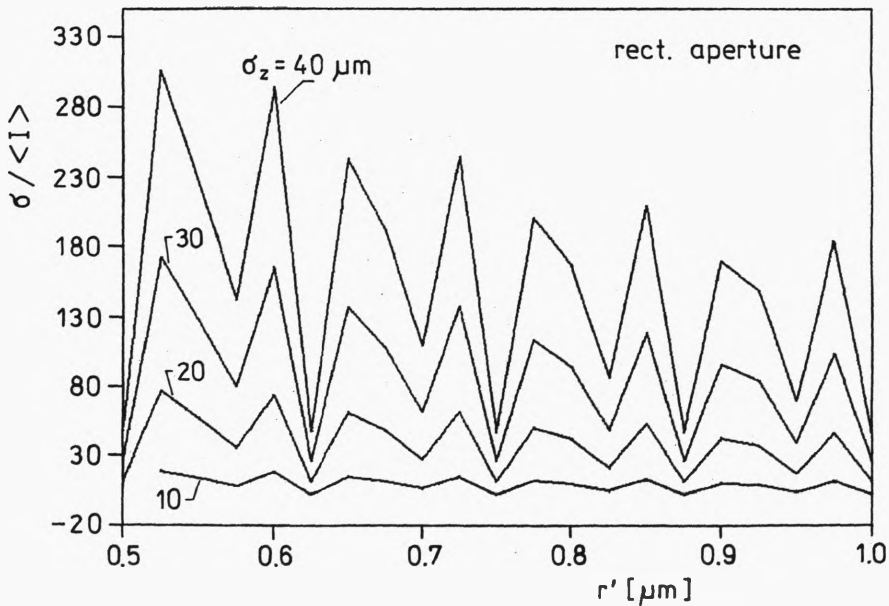
Fig. 6. Set of four curves of the normalized intensity $\sigma/\langle I \rangle$ vs. the radial coordinate r' [μm] of the far-field speckle pattern, where r' ranges from 0.0 μm up to 0.5 μm, NA = 0.5, BW = 10 nm, and σ_z = 10, 20, 30, 40 μm. NA is the numerical aperture of the diaphragm that limits the diffuser

Fig. 7. Set of four curves of the normalized intensity $\sigma/\langle I \rangle$ vs. the radial coordinate r' [μm] of the far-field speckle pattern, where r' ranges from 0.5 μm up to 1.0 μm, NA = 0.5, BW = 10 nm, σ_z = 10, 20, 30, 40 μm. NA is the numerical aperture
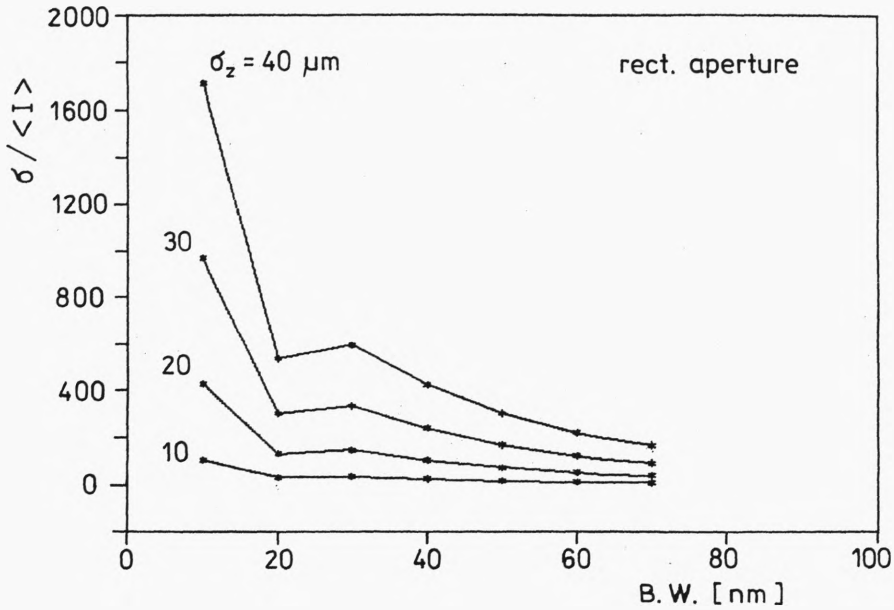
Fig. 8. Set of four curves of the normalized intensity $\sigma/\langle I \rangle$ vs. the bandwidth β [nm] of the far-field speckle pattern near the origin at $r' = 0.1\ \mu m$, NA = 0.5, and $\sigma_z = 10, 20, 30$ and $40\ \mu m$. NA — numerical aperture of the diaphragm that limits the diffuser
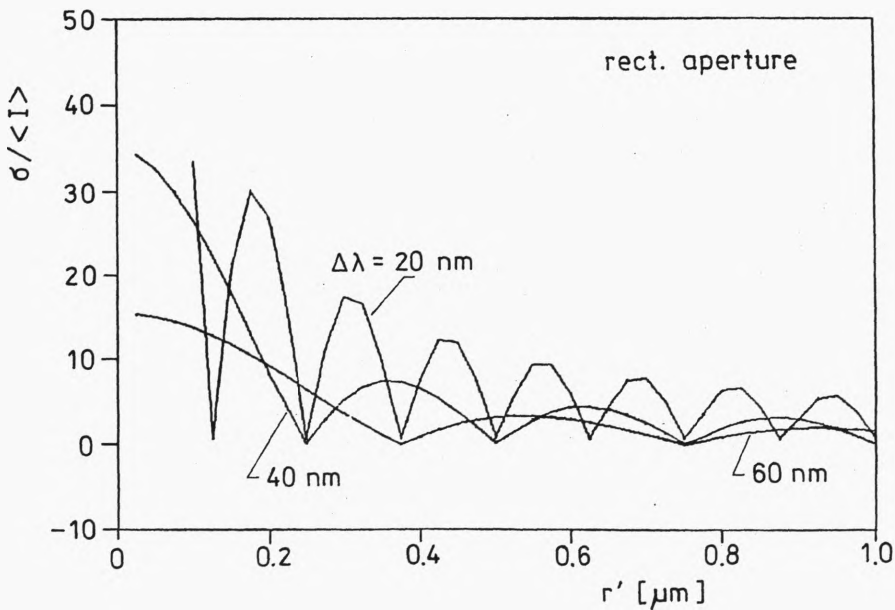

Fig. 9. Normalized values of $\sigma/\langle I \rangle$ vs. r' [μm] measured outside the stationary region. Curves are shown for $\sigma_z = 10\ \mu m$ at different bandwidths of the incident light

Figs. 1−7, that the intensities in all the curves oscillate between higher values at the centre of the speckle pattern and lower values outside the origin for certain r.m.s. surface roughness. For example, $\sigma/\langle I \rangle = 1700$ units near the centre, while it is only 300 units at $r' = 1.0$ μm and $\sigma_z = 40$ μm as compared with $\sigma/\langle I \rangle = 110$ units near the origin and zero at $r' = 1.0$ μm and $\sigma_z = 5$ μm. Referring to Fig. 3, it is shown that a slight variation in the ratio $\sigma/\langle I \rangle$ occurs outside the stationary region for $\sigma_z \leqslant 10$ μm. Figure 8 shows $\sigma/\langle I \rangle$ of the far-field speckle pattern variation versus the
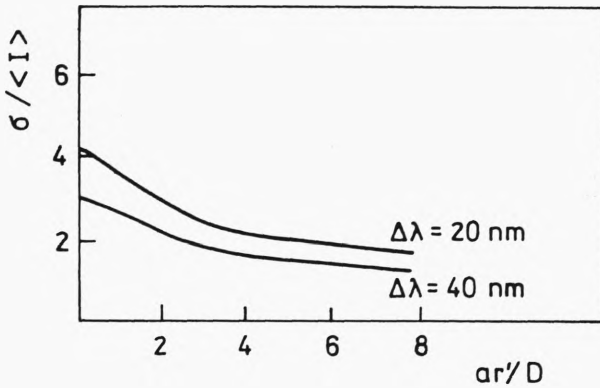

Fig. 10. Parry results [17] representing the ratio $\sigma/\langle I \rangle$ vs. ar'/D. The aperture has a uniform circular shape. Curves are shown for $\sigma_z = 10$ μm at different bandwidths of the incident light
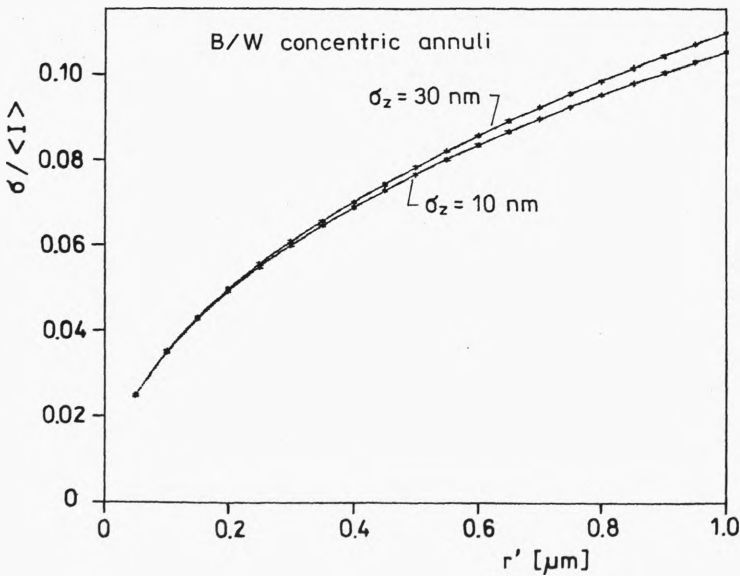

Fig. 11. Normalized irradiance $\sigma/\langle I \rangle$ vs. the radial coordinate r' of the speckle pattern using a modulated aperture composed of black and transparent concentric annuli

bandwidth β near the origin at $r' = 0.1$ μm. Four curves are plotted corresponding to four different values of $\sigma_z = 10, 20, 30$ and 40 μm. It is clear from the results obtained in this case that the ratio $\sigma/\langle I \rangle$ is nearly invariant for smaller values of r.m.s. surface roughness $\sigma_z \leqslant 10$ μm, while an abrupt change occurs for higher values of surface roughness $\sigma_z = 40$ μm in the range $\beta = 10-20$ nm and then increases slightly in the range from 20 up to 30 nm, and then a smooth nonlinear variation occurs in the range $30-70$ nm. Figure 9 shows three different curves of the ratio $\sigma/\langle I \rangle$ versus r' at certain value of $\sigma_z = 10$ μm. It is clear that the oscillating variation increases for smaller values of $\Delta \lambda = 20$ nm, while it is decreased for greater values of $\Delta \lambda = 60$ nm. Hence, finer details are shown for narrower bandwidth leading to an improvement in image contrast of the speckle pattern. Figure 10 which is obtained for uniform circular aperture [17] is plotted to be compared with the results represented in Fig. 9. Figure 11 shows two curves of the normalized values of the ratio $\sigma/\langle I \rangle$ versus the radial coordinate r', considering a modulated aperture composed of B/W concentric annuli represented in Fig. 2 and $\sigma_z = 30, 40$ μm. It is shown that the ratio $\sigma/\langle I \rangle$ is gradually increased outside the stationary region. It should be noted that the numerical aperture (NA) of the diaphragm that limits the diffuser is set equal to 0.5.

4. Conclusion

It is shown that the normalized values of $\sigma/\langle I \rangle$ versus the radial coordinate of the speckle pattern may be exploited to improve the image contrast of the speckle pattern using both a narrow bandwidth and a rectangular aperture limiting the diffuser. The B/W concentric annuli used as an aperture limiting the diffuser show that the ratio $\sigma/\langle I \rangle$ may be improved outside the origin of the speckle pattern. Consequently, this work may be applied to study different types of diffusers using modulated apertures in order to improve the ratio $\sigma/\langle I \rangle$.

References

[1] GOODMAN J. W., Stanford Electronics Lab. Tech. Report (1963), No. 2303 − 1.
[2] GOODMAN J. W., Proc. IEEE **53** (1965), 1688.
[3] ENLOE L. M., Bell Syst. Tech. J. **46** (1967), 1479.
[4] DAINTY J. C., Opt. Acta **17** (1970), 761.
[5] DAINTY J. C., Opt. Acta **18** (1971), 327.
[6] ELBAUM M., GREENBAUM M., KING M., Opt. Commun. **5** (1972), 171.
[7] BARAKAT R., Opt. Acta. **20** (1973), 729.
[8] SPRAGUE R. A., Appl. Opt. **11** (1972), 2811.
[9] FUJI H., ASAKURA T., Opt. Commun. **11** (1974), 35.
[10] FUJI H., ASAKURA T., Opt. Commun. **12** (1974), 32.
[11] FUJI H., ASAKURA T., Nouv. Rev. Opt. **6** (1975), 5.
[12] OHTSUBO J., ASAKURA T., Nouv. Rev. Opt. **6** (1975), 189.
[13] OHTSUBO J., ASAKURA T., Opt. Commun. **14** (1975), 30.
[14] FUJI H., ASAKURA T., SHINDO Y., Opt. Commun. **16** (1976), 68.
[15] FUJI H., UOZUMI J., ASAKURA T., J. Opt. Soc. Am. **66** (1976), 1222.
[16] HAMED A. M., EL-SHABSHIRY M., Opt. Appl. **13** (1983), 317.

[17] PARRY G., Opt. Acta **21** (1974), 763.
[18] PEDERSEN H. M., Opt. Acta **22** (1975), 15.
[19] PEDERSEN H. M., J. Opt. Soc. Am. **66** (1976), 1204.
[20] PEDERSEN H. M., Opt. Commun. **16** (1976), 63.
[21] PEDERSEN H. M., Opt. Acta **22** (1975), 523.
[22] REED I. S., IRE Trans. Inf. Theory **8** (1962), 194.
[23] HAMED A. M., CLAIR J. J., Optik **64** (1983), 277.
[24] FRANCON M., Opt. Acta **20** (1973), 1.